

Controlling electron motion with attosecond precision by shaped femtosecond intense laser pulse

XIAOYUN ZHAO^{1,†}, MINGQING LIU^{2,†}, YIZHANG YANG³, ZHOU CHEN³,
XIAOLEI HAO^{1,6}, CHUNCHENG WANG^{3,7}, WEIDONG LI⁴, JING
CHEN^{4,5,8}

¹*Institute of Theoretical Physics and Department of Physics, State Key Laboratory of Quantum Optics and Quantum Optics Devices, Collaborative Innovation Center of Extreme Optics, Shanxi University, Taiyuan 030006, China*

²*School of Physics and Information Technology, Shaanxi Normal University, Xi'an 710119, China*

³*Institute of Atomic and Molecular Physics and Jilin Provincial Key Laboratory of Applied Atomic and Molecular Spectroscopy, Jilin University, Changchun 130012, China*

⁴*Shenzhen Key Laboratory of University Laser and Advanced Material Technology, Center for Advanced Material Diagnostic Technology, and College of Engineering Physics, Shenzhen Technology University, Shenzhen 518118, China*

⁵*Hefei National Laboratory, Department of Modern Physics, University of Science and Technology of China, Hefei 230026, China*

[†]*These authors contribute equally to this work.*

⁶*xlhao@sxu.edu.cn*

⁷*ccwang@jlu.edu.cn*

⁸*chenjing@ustc.edu.cn*

Abstract: We propose the scheme of temporal double-slit interferometer to precisely measure the electric field of shaped intense femtosecond laser pulse directly, and apply it to control the electron tunneling wave packets in attosecond precision. By manipulating the spectra phase of the input femtosecond pulse in frequency domain, one single pulse is split into two sub-pulses whose waveform can be precisely controlled by adjusting the spectra phase. When the shaped pulse interacts with atoms, the two sub-pulses are analogous to the Young's double-slit in time domain. The interference pattern in the photoelectron momentum distribution can be used to precisely retrieve the peak electric field and the time delay between two sub-pulses. Based on the precise characterization of the shaped pulse, we demonstrate that the sub-cycle dynamics of electron can be controlled with attosecond precision. The above scheme is proved to be feasible by both quantum-trajectory Monte Carlo simulations and numerical solutions of three-dimensional time-dependent Schrödinger equation.

© 2023 Optical Society of America under the terms of the [OSA Open Access Publishing Agreement](#)

1. INTRODUCTION

Precise control of electron motion in atoms or molecules became accessible since the advent of laser. Considering the time scale of electron motion, femtosecond or even attosecond lasers are indispensable to modulate electron dynamics [1–4]. One can directly change the parameter of a single laser [5–8], or construct a pump-probe scheme by varying the time delay between two femtosecond lasers [9–11] or one femtosecond laser plus one attosecond laser [12–17]. Recently, direct combining two-color laser fields to form a shaped laser field in temporal domain [18–22], which can be controlled by varying the parameters of the two lasers, is applied to modulate the motion of tunneling electron wave packets. On the other hand, the technology of femtosecond pulse shaping [23, 24], in which Fourier synthesis methods are used to generate nearly arbitrarily shaped ultrafast optical wave forms with a single laser, has been successfully developed to

manipulate the evolution of a quantum system [25, 26] and thus control various atomic and molecular processes such as the high harmonic generation [27, 28], the strong-field ionization of molecules [29, 30].

How precise the control of electron dynamics can be achieved not only depends on how subtly we can change the laser field but also depends on how accurately we can characterize it. Since the electron dynamics is sensitive to the temporal shape of the laser field [19, 31], to control the electron dynamics in attosecond precision puts higher requirements to the control and measurement of the laser field in time domain. Femtosecond pulse shaping is an ideal candidate due to its capability of temporally reshaping the laser field in a very precise and flexible manner. However, to directly measure the tailored laser field is still a challenge, which prevents the further control of electron motion in a precise way. In practice, the shaped laser field is reconstructed based on the information of the input laser which are equally difficult to be measured accurately enough. As a result, the shaped laser field can only be estimated in a largely uncertain way which is far from the requirements. In this work, by introducing the temporal double-slit interferometer, we propose a scheme to directly measure the shaped laser field in an unprecedented precision. Based on this, control of the electron tunneling wave packets in attosecond resolution with shaped femtosecond laser pulse is achieved.

2. Results and discussions

As illustrated in Fig. 1, a conventional single femtosecond intense laser pulse can be shaped into a pair of sub-pulses by adding a phase of π in the spectra from specific wavelength λ_s in frequency domain. The shape of the output pulse, which is mainly determined by the amplitude of the two sub-pulses and the time delay between them, can be controlled by adjusting λ_s . The shaped laser field corresponding to specific λ_s is measured based on the principle of Young's double-slit interference in time domain. The basic idea behind it is as follows. If atoms are exposed to unshaped single intense laser pulse, they will be ionized and exhibit a typical photoelectron momentum distribution (PMD) characterized by a series of above-threshold ionization (ATI) rings separated by one photon energy [6] as shown in Fig. 1(a). Meanwhile, the ATI ring displays stripes at specific angles, known as jet-like structure. When the shaped pulse is used to ionize atoms, the photoelectrons born in the two sub-pulses will interfere, resulting in the ATI ring to split into several sub-rings [see Fig. 1(b)], while the jet-like structure survives. The amplitude and the time delay of the two sub-pulses can be retrieved based on positions and fringe spacing of the sub-rings, just like what is done in Young's double-slit experiment for light. We call this technique temporal Young's double-slit interferometer. Then, by varying λ_s , very subtle changes of the shape of the tailored pulse can be characterized. With this capability, we can manipulate the electron tunneling dynamics in attosecond precision.

Before that, we shall first demonstrate that the sub-ring structure in Fig. 1(b) calculated with quantum trajectory Monte Carlo (QTMC) method is indeed the result of the interference of ionization events from different sub-pulses. In simulations of QTMC [32, 33] (see supplement 1 for details), we can explicitly obtain the PMD corresponding to ionization events born in selected range of time in the shaped pulse. If the ionization is confined to a single sub-pulse [for example, $t_i < 0$ in Fig. 2(a1)], the PMD shows similar features to the case of the unshaped pulse: clear ATI rings without splitting are modulated with a jet-like structure [within white dashed lines in Fig. 2(b)]. The ATI rings with spacing of one photon energy are usually recognized as the result of interference between electrons ionized in adjacent optical cycles, termed as intercycle interference [34]. The jet-like structure can be attributed to the interference of electrons ionized in an optical cycle [32], known as intracycle interference [35]. As sketched in Fig. 2(a2), electrons emitted at times t_{i1} and t_{i2} possess an identical final momentum of $\mathbf{p} = -\mathbf{A}(t_i)$, where $\mathbf{A}(t)$ is the vector potential, and subsequently, they will interfere. This can be demonstrated explicitly by considering electrons ionized within only one optical cycle [the region in dashed

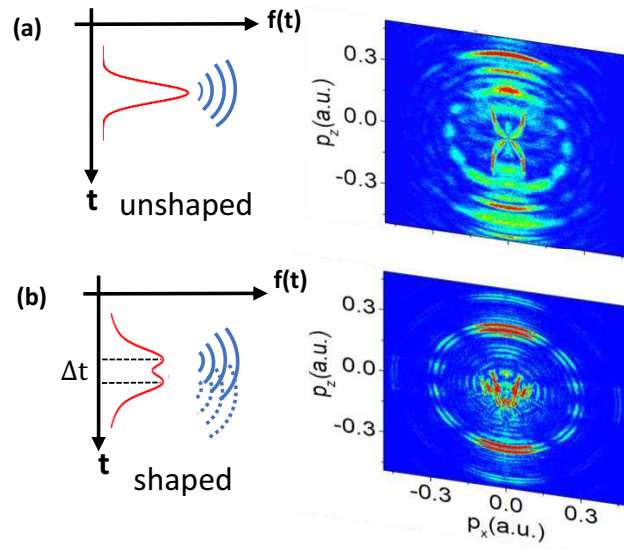


Fig. 1. Sketch maps for ionization processes if Xe atoms are exposed to the unshaped single pulse (a) and to the shaped pulse with the time delay of Δt between the two sub-pulses (b). The photoelectron momentum distributions (PMDs) are simulated by quantum trajectory Monte Carlo (QTMC) method. The laser intensity of the input unshaped pulse is $I_0 = 1.5 \times 10^{14}$ W/cm², the central wavelength is $\lambda_0 = 800$ nm, and the pulse duration is 20 fs.

box in Fig. 2(a1)], as shown in Fig. 2(c), in which intracycle interference causes the jet-like structure to prevail in the PMD.

Figure 2(b) suggests that ionizations in both sub-pulses are necessary for the formation of the sub-ring structure. Then, if the ionization times are limited in two symmetric half-optical-cycles in the negative direction around the envelope maximum of each sub-pulse [green regions in Fig. 2(a1)], the interference of electrons ionized in these two regions generates a multitude of rings as shown in Fig. 2(d). The spacing of these rings matches that of the sub-ring structure in Fig. 1(b). Further, when electrons originating from adjacent half-optical-cycles in negative field direction [blue regions in Fig. 2(a1)] are also involved, adjacent intercycle interference comes into play and the sub-ring structure is modulated by ATI rings [see Fig. 2(e)]. Finally, after adding electrons ionized in the positive electric field [red regions in Fig. 2(a1)], intracycle interference occurs and the jet-like structure [within white dashed lines in Fig. 2(f)] is formed. This almost reproduces the complete PMD for the shaped pulse in Fig. 1(b). It can therefore be concluded that the sub-ring structure in the PMD of the shaped pulse is induced by interference between the electrons ionized in the two sub-pulses, that is, double-slit interference in the time domain. Moreover, in Fig. 2(g), we also present simulated PMD by numerically solving three-dimensional time-dependent Schrödinger equation (TDSE) [36, 37] (see supplement 1 for details of the method). The same laser parameters as that in QTMC calculations are applied. The TDSE-simulated PMD, which also features split ATI rings along with a jet-like structure [within white dashed lines in Fig. 2(g)], exhibits excellent agreement with the QTMC results presented in Fig. 2(g) and Fig. 1(b).

Based on the principle of Young's double-slit interference, the interference fringes in the PMD are used to retrieve the peak field and time delay of the shaped pulse constituted of two sub-pulses. The interference fringe spacing is straitly related to the time delay between the two

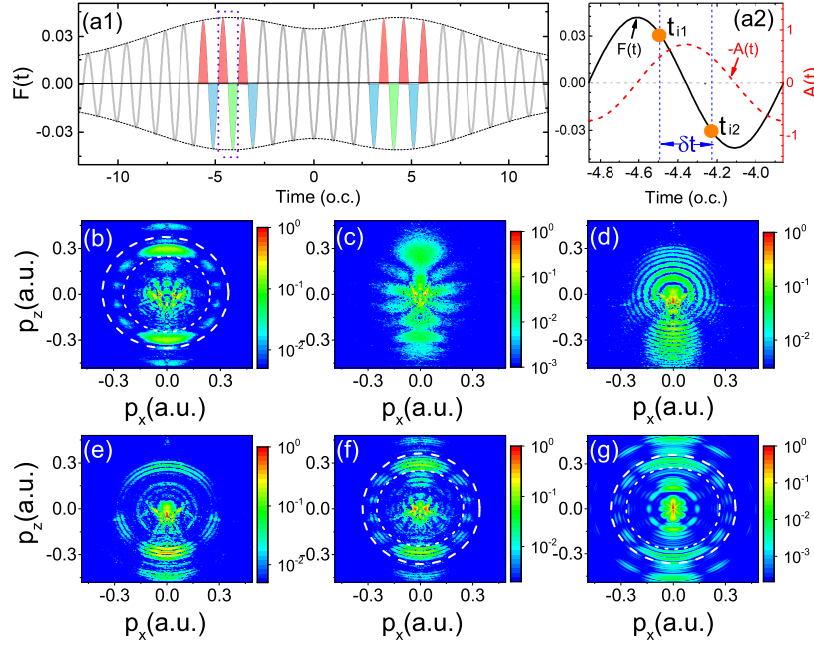


Fig. 2. (a1): The electric field $F(t)$ of the shaped pulse as a function of time. (a2): The electric field and the negative vector potential $-A(t)$ within one optical cycle indicated by violet dashed rectangle as shown in panel (a1), t_{i1} and t_{i2} denote the ionization times of intracycle interference trajectories which have the same final momentum with time difference δt . Simulated PMDs by QTMC are obtained by considering electrons ionized at different time ranges: (b) $t_i < 0$, (c) t_i in a single optical cycle enclosed by the dashed rectangle, (d) t_i in green regions, (e) t_i in green and blue regions, (f) t_i in green, blue, and red regions. (g): PMD calculated by numerically solving three-dimensional time-dependent Schrödinger equation (TDSE). The white dashed lines are used to indicate the sub-ring and jet-like structure. $\lambda_s = 780$ nm and the other pulse parameters are the same as in Fig. 1.

sub-pulses. The relation can be obtained based on strong field approximation (SFA) [38]. For electron ionized at time t_i with final momentum \mathbf{p} , the phase is given by the classical action in atomic units ($\hbar = m_e = e = 1$)

$$S(\mathbf{p}, t_i) = \int_{t_i}^{\infty} dt \left(\frac{1}{2} [\mathbf{p} + \mathbf{A}(t)]^2 + I_p \right), \quad (1)$$

where $\mathbf{A}(t)$ is the vector potential, I_p is the binding potential. The interference fringe occurs when the phase difference between electrons ionized around the two envelope maxima of the shaped pulse reaches $2m\pi$ (m is an integer), that is (see supplement 1 for details)

$$(E + I_p + U_p)\Delta t - \frac{U_p}{\omega_0} \sin(\omega_0 \Delta t) = 2m\pi, \quad (2)$$

where $E = p^2/2$ is the electron energy, $U_p = F_0^2/4\omega_0^2$ is the pondermotive potential (F_0 is the peak electric field of the sub-pulse and ω_0 is the optical central frequency), Δt is the difference of the ionization time which is equal to the time delay between the two sub-pulses. When the electron energy varies ΔE which is just equal to the fringe spacing of the sub-ring structure in

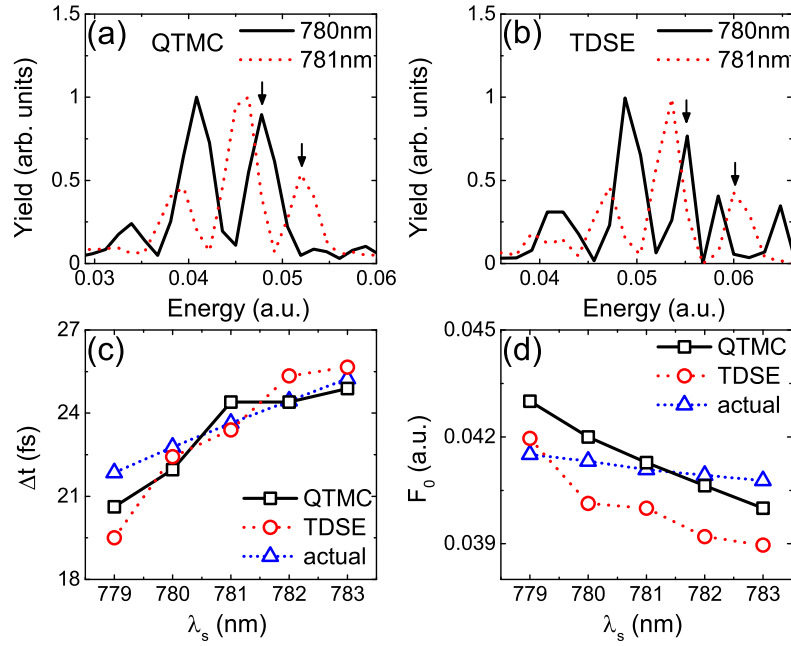


Fig. 3. Energy spectra for shaped pulses simulated by QTMC (a) and TDSE (b), and the corresponding extracted time delay Δt (c) and peak electric field strength F_0 (d) of the shaped pulse at different λ_s . The actual values of Δt and F_0 are also presented for comparison. The arrows in panels (a) and (b) are used to indicate the sub-ring used in Fig. 4.

the PMD, the phase difference will change 2π . Then the time delay between the two sub-pulses can be estimated as

$$\Delta t = 2\pi/\Delta E. \quad (3)$$

Therefore, we only have to read the fringe spacing in the PMD to obtain the time delay. Furthermore, if we know the exact value of m in Eq. (2), we can determine U_p and thus determine the peak electric field F_0 of the shaped pulse. This can be achieved with help of the jet-like structure of the PMD. The jet-like structure has been widely discussed previously and can be explained by either multiphoton ionization or sub-cycle electron wave-packet interference [39, 40]. The nodes of the jet-like structure on the ATI ring is closely related to the number of photons the electron absorbs. The case of 10 nodes in Fig. 1(b) corresponds to 11-photon channel. We can deduce a guessed U_p according to the energy conservation: $n\omega_0 - I_p - U_p = E$, which describes that a bounded electron absorbs n photons to overcome the binding potential I_p plus the pondermotive potential U_p and eventually becomes a free electron with energy E . Then we substitute the guessed U_p into Eq. (2) to make correction to it by ensuring that m is an integer. Eventually, both the peak electric field and the time delay of the two sub-pulse are obtained for specific λ_s . If varying λ_s , the shape of the tailored laser field will change accordingly, resulting in the shift of the interference fringes and the change of the fringe spacing. This can be seen clearly in the angle-integrated energy spectra simulated by both QTMC [Fig. 3(a)] and TDSE [Fig. 3(b)] methods, in which the peaks shift to the right and the spacing between them decreases when λ_s increases. Applying the temporal Young's double-slit interferometer, Δt and F_0 for different λ_s are extracted from the simulated photoelectron spectra, as shown in Fig. 3(c) and Fig. 3(d). For comparison, we also present the actual values read directly from the shaped pulse.

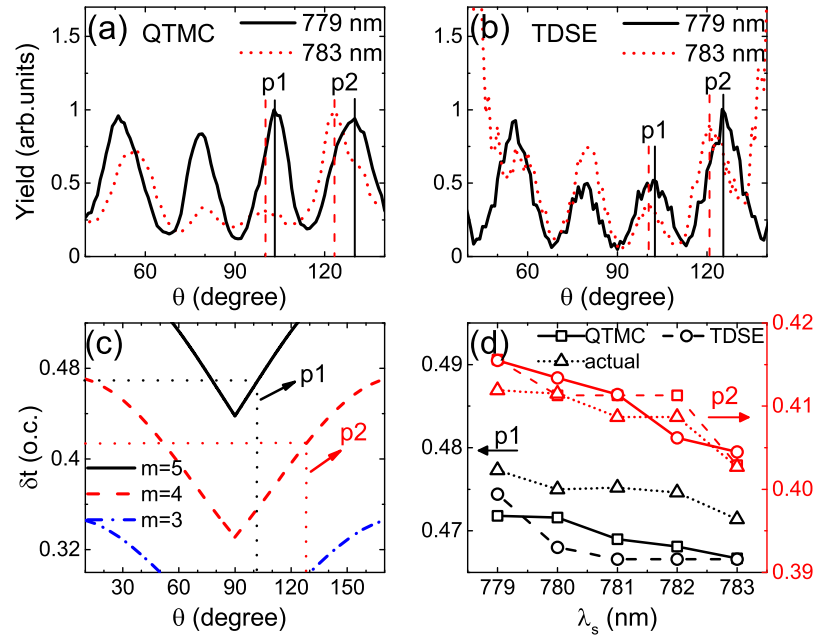


Fig. 4. Angular distribution corresponding to a specific sub-ring at different λ_s simulated by QTMC (a) and TDSE (b). The positions for peaks $p1$ and $p2$ are indicated by vertical lines. Panel (c) shows the curves obtained from Eq. (4), and illustrates how the ionization time difference δt between the two interfering electron trajectories contributing to the two peaks (labelled as $p1$ and $p2$) in panels (a) and (b) can be extracted from the curves. (d) The extracted λ_s -dependent δt corresponding to peaks $p1$ and $p2$. The actual values of δt obtained through statistics of the trajectories in the QTMC simulations are also presented for comparison. The sub-rings used above are indicated by arrows in Figs. 3(a) and 3(b).

The retrieved results for both QTMC and TDSE are found to be in good agreement with the actual values, which proves the accuracy of the interferometer. Even better, it needs only to obtain the slope of the λ_s dependence with some raw data points in real experiments, since the time delay and peak electric field vary with λ_s almost linearly. For example, the slope of the time delay vs λ_s in Fig. 3(c) is approximately 1097 as/nm, then for the shortest step of adjusting λ_s that can be achieved, i.e., 0.2 nm, the corresponding step of the time delay is 220 as.

After accurate characterization of the electric-field waveform of the shaped pulse, the precise control of electronic dynamics becomes possible. Actually, the λ_s -dependent sub-ring structure in the PMD has demonstrated the capacity of the shaped pulse to control the dynamics of the tunneling wave packets. However, since the sub-ring structure is the result of intercycle interference, the precision of this kind of manipulation of the electron motion is limited to half the optical cycle (1.3 fs for an 800 nm laser), although the precision of modulating the time delay between the two sub-pulses can be achieved on the attosecond scale. In fact, along with the ability to control the time delay of the shaped pulse, we can also precisely modulate its peak electric field strength concurrently [see Fig. 3(d)]. Here, we will exploit the latter capability to control the electron sub-cycle dynamics with attosecond precision. For this purpose, let us turn to the angular distribution featured with a series of peaks corresponding to the jet-like structure in the PMD, which is sensitive to the peak electric field. Examining the jet-like structure for a specific sub-ring, we find that the peaks in the photoelectron angular distribution simulated

by both TDSE and QTMC shrink towards 90 degrees (perpendicular to the laser polarization) with increasing λ_s , as shown in Figs. 4(a) and 4(b). Since the jet-like structure is the result of intracycle interference, its evolution with λ_s indicates the possibility of manipulating the electron dynamics with sub-cycle precision. This sub-cycle dynamic is characterised by δt , the difference in ionization time for the two interfering electron trajectories born within an optical cycle as sketched in Fig. 2(a2), which can be extracted from the angular distribution by phase analysis based on Eq. (1). The peak at a specific angle θ in the angular distribution occurs when the phase difference between the two trajectories experiencing intracycle interference reaches $2m\pi$, which gives the following relationship (see supplement 1 for details)

$$(E + I_p + U_p)\delta t - \frac{\sqrt{2EF_0}}{\omega_0^2} |\cos \theta| \sin\left(\frac{\omega_0}{2}\delta t\right) - \frac{U_p}{\omega_0} \sin(\omega_0\delta t) = 2m\pi. \quad (4)$$

As long as the photoelectron energy E and the peak electric field strength F_0 are specified, the above relationship between δt and θ for certain m is determined. Here, this relationship is established using the mean values of E and F_0 at different λ_s . The curves given by Eq. (4) are shown in Fig. 4(c), from which δt can be directly extracted. According to the phase analysis, if we count the number of peaks in the angular distribution starting from 90 degrees, the first peak corresponds to the largest m that Eq. (4) allows, the second peak corresponds to $m - 1$, and so on. Therefore, δt for peak $p1$ in Fig. 4(a) should be extracted from the curve of $m = 5$, and δt for peak $p2$ should be read from the curve of $m = 4$, as illustrated in Fig. 4(c). In Fig. 4(d), we present the δt extracted from spectra simulated by QTMC and TDSE at different λ_s , which exhibits a monotonously decreasing dependence on λ_s . We also provide the actual values of δt obtained through statistics of the trajectories contributing to the peaks in the QTMC simulations. The good agreement between the extracted δt for both QTMC and TDSE with the actual values supports the validity of the extraction method. Note that there is a greater discrepancy between the extracted and actual values for peak $p1$ compared to peak $p2$. This is due to the fact that the additional rescattering trajectories not considered in Eq. (4) are involved in the formation of peak $p1$ [32], which will affect the extracted results. The results in Fig. 4(d) clearly demonstrate that the sub-cycle electronic dynamics, characterized by δt , can be manipulated with attosecond precision by regulating the shaped laser field. The slope of the regulation curve for δt extracted from peak $p1$ and peak $p2$ is approximately 4 and 7 as/nm, respectively.

3. Conclusions

In summary, we proposed a temporal Young's double-slit interferometer to characterize the shaped laser field with unprecedented precision. By reversing the phase of the frequency spectra from specific wavelength λ_s , a conventional single femtosecond pulse is split into a pair of sub-pulses in time domain after Fourier transformation, whose shape can be precisely controlled by adjusting λ_s . Based on the principle of Young's double-slit interference in time domain, in which the two sub-pulses are analogous to the double-slit, the peak electric field and the time delay between them can be precisely retrieved from the interference pattern in PMD resulted from the interaction of shaped pulse with atoms. With this capability, we show that the sub-cycle dynamics of electron can be controlled with shaped pulse and the precision of control is in attosecond scale. The above scheme is proved to be feasible by both QTMC and TDSE simulations. It is worthy to note that the shaped pulse consisting of two sub-pulses can also be regarded as the construction of a pump-probe scheme. Our work demonstrates that the time delay between the pump and probe pulses can be manipulated in attosecond precision. In addition, the proposed scheme can also be extended to circularly polarized laser field to combine with the technology of attoclock, which may be capable of probing and controlling electronic dynamics with even higher precision.

Funding.

This work was supported by the National Key Research and Development Program (No. 2019YFA0307700), the National Natural Science Foundation of China (No. 12274273, No. 12204314, No. 92261201, No. 12274179), the Innovation Program for Quantum Science and Technology (No. 2021ZD0302101) and the Natural and Science Foundation of Top Talent of SZTU(No. GDRC202202).

Disclosure.

The authors declare no conflicts of interest.

Data availability.

Data underlying the results presented in this paper are not publicly available at this time but may be obtained from the authors upon reasonable request.

Supplemental document.

See Supplement 1 for supporting content.

References

1. H. Niikura, F. Légaré, R. Hasbani, A. D. Bandrauk, M. Y. Ivanov, D. M. Villeneuve, and P. B. Corkum, "Sublaser-cycle electron pulses for probing molecular dynamics," *Nature* **417**, 917-922 (2002).
2. E. Goulielmakis, Z.-H. Loh, A. Wirth, R. Santra, N. Rohringer, V. S. Yakovlev, S. Zherebtsov, T. Pfeifer, A. M. Azzeer, M. F. Kling, S. R. Leone, and F. Krausz, "Real-time observation of valence electron motion," *Nature* **466**, 739-743 (2010).
3. A. Baltuška, T. Udem, M. Uiberacker, M. Hentschel, E. Goulielmakis, C. Gohle, R. Holzwarth, V. S. Yakovlev, A. Scrinzi, T. W. Hänsch, and F. Krausz, "Attosecond control of electronic processes by intense light fields," *Nature* **421**, 611-615 (2003).
4. S. R. Leone, C. W. McCurdy, J. Burgdörfer, L. S. Cederbaum, Z. Chang, N. Dudovich, J. Feist, C. H. Greene, M. Ivanov, R. Kienberger, U. Keller, M. F. Kling, Z.-H. Loh, T. Pfeifer, A. N. Pfeiffer, R. Santra, K. Schafer, A. Stolow, U. Thumm, and M. J. J. Vrakking, "What will it take to observe processes in 'real time'?", *Nat. Photonics* **8**, 162-166 (2014).
5. G. G. Paulus, F. Lindner, H. Walther, A. Baltuška, E. Goulielmakis, M. Lezius, and F. Krausz, "Measurement of the phase of few-cycle laser pulses," *Phys. Rev. Lett.* **91**, 253004 (2003).
6. C. M. Maharjan, A. S. Alnaser, I. Litvinyuk, P. Ranitovic, and C. L. Cocke, "Wavelength dependence of momentum-space images of low-energy electrons generated by short intense laser pulses at high intensities," *J. Phys. B* **39**, 1955 (2006).
7. H. Kang, K. Henrichs, M. Kunitski, Y. Wang, X. Hao, K. Fehre, A. Czasch, S. Eckart, L. Schmidt, M. Schöffler, T. Jahnke, X. Liu, and R. Dörner, "Timing recollision in nonsequential double ionization by intense elliptically polarized laser pulses," *Phys. Rev. Lett.* **120**, 223204 (2018).
8. C. I. Blaga, F. Catoire, P. Colosimo, G. G. Paulus, H. G. Muller, P. Agostini, and L. F. DiMauro, "Strong-field photoionization revisited," *Nat. Phys.* **5**, 335-338 (2009).
9. A. H. Zewail, "Laser femtochemistry," *Science* **242**, 1645-1653 (1988).
10. A. H. Zewail, "Femtochemistry: atomic-scale dynamics of the chemical bond," *J. Phys. Chem. A* **104**, 5660-5694 (2000).
11. M. Dantus, R. M. Bowman, and A. H. Zewail, "Femtosecond laser observations of molecular vibration and rotation," *Nature* **343**, 737-739 (1990).
12. D. Huh, B. D. Matthews, A. Mammoto, M. Montoya-Zavala, H. Y. Hsin, and D. E. Ingber, "Reconstituting organ-level lung functions on a chip," *Science* **328**, 1662-1668 (2010).
13. A. L. Cavalieri, N. Müller, T. Uphues, V. S. Yakovlev, A. Baltuška, B. Horvath, B. Schmidt, L. Blümel, R. Holzwarth, S. Hendl, M. Drescher, U. Kleineberg, P. M. Echenique, R. Kienberger, F. Krausz, and U. Heinzmann, "Attosecond spectroscopy in condensed matter," *Nature* **449**, 1029-1032 (2007).
14. K. Klünder, J. M. Dahlström, M. Gisselbrecht, T. Fordell, M. Swoboda, D. Guénot, P. Johnsson, J. Caillat, J. Mauritsson, A. Maquet, R. Taïeb, and A. L'uillier, "Probing single-photon ionization on the attosecond time scale," *Phys. Rev. Lett.* **106**, 143002 (2011).
15. M. Ossiander, F. Siegrist, V. Shirvanyan, R. Pazourek, A. Sommer, T. Latka, A. Guggenmos, S. Nagele, J. Feist, J. Burgdörfer, R. Kienberger, and M. Schultze, "Attosecond correlation dynamics," *Nat. Phys.* **13**, 280-185 (2016).
16. M. Swoboda, T. Fordell, K. Klünder, J. M. Dahlström, M. Miranda, C. Buth, K. J. Schafer, J. Mauritsson, A. L'Huillier, and M. Gisselbrecht, "Phase measurement of resonant two-photon ionization in helium," *Phys. Rev. Lett.* **104**, 103003 (2010).

17. X. Gong, W. Jiang, J. Tong, J. Qiang, P. Lu, H. Ni, R. Lucchese, K. Ueda, and J. Wu, "Asymmetric attosecond photoionization in molecular shape resonance," *Phys. Rev. X* **12**, 011002 (2022).
18. C. A. Mancuso, D. D. Hickstein, P. Grychtol, R. Knut, O. Kfir, X.-M. Tong, F. Dollar, D. Zusin, M. Gopalakrishnan, C. Gentry, E. Turgut, J. L. Ellis, M.-C. Chen, A. Fleischer, O. Cohen, H. C. Kapteyn, and M. M. Murnane, "Strong-field ionization with two-color circularly polarized laser fields," *Phys. Rev. A* **91**, 031402 (2015).
19. K. Lin, X. Jia, Z. Yu, F. He, J. Ma, H. Li, X. Gong, Q. Song, Q. Ji, W. Zhang, H. Li, P. Lu, H. Zeng, J. Chen, and J. Wu, "Comparison study of strong-field ionization of molecules and atoms by bicircular two-color femtosecond laser pulses," *Phys. Rev. Lett.* **119**, 203202 (2017).
20. S. Eckart, M. Kunitski, I. Ivanov, M. Richter, K. Fehre, A. Hartung, J. Rist, K. Henrichs, D. Trabert, N. Schlott, L. P. H. Schmidt, T. Jahnke, M. S. Schöffler, A. Kheifets, and R. Dörner, "Subcycle interference upon tunnel ionization by counter-rotating two-color fields," *Phys. Rev. A* **97**, 041402 (2018).
21. M. Han, P. Ge, M.-M. Liu, Q. Gong, and Y. Liu, "Spatially and temporally controlling electron spin polarization in strong-field ionization using orthogonal two-color laser fields," *Phys. Rev. A* **99**, 023404 (2019).
22. D. B. Milošević, W. Becker, and R. Kopold, "Generation of circularly polarized high-order harmonics by two-color coplanar field mixing," *Phys. Rev. A* **61**, 063403 (2000).
23. A. Weiner, "Femtosecond optical pulse shaping and processing," *Prog. Quant. Electron.* **19**, 161-237 (1995).
24. A. M. Weiner, "Femtosecond pulse shaping using spatial light modulators," *Rev. Sci. Instrum.* **71**, 1929-1960 (2000).
25. T. Brixner, G. Krampert, T. Pfeifer, R. Selle, G. Gerber, M. Wollenhaupt, O. Graefe, C. Horn, D. Liese, and T. Baumert, "Quantum control by ultrafast polarization shaping," *Phys. Rev. Lett.* **92**, 208301 (2004).
26. N. Dudovich, D. Oron, and Y. Silberberg, "Quantum control of the angular momentum distribution in multiphoton absorption processes," *Phys. Rev. Lett.* **92**, 103003 (2004).
27. R. Bartels, S. Backus, E. Zeek, L. Misoguti, G. Vdovin, I. P. Christov, M. M. Murnane, and H. C. Kapteyn, "Shaped-pulse optimization of coherent emission of highharmonic soft x-rays," *Nature* **406**, 164-166 (2000).
28. D. Oron, Y. Silberberg, N. Dudovich, and D. M. Villeneuve, "Efficient polarization gating of high-order harmonic generation by polarization-shaped ultrashort pulses," *Phys. Rev. A* **72**, 063816 (2006).
29. V. Tagliamonti, B. Kaufman, A. Zhao, T. Rozgonyi, P. Marquetand, and T. Weinacht, "Time-resolved measurement of internal conversion dynamics in strong-field molecular ionization," *Phys. Rev. A* **96**, 021401 (2017).
30. B. Kaufman, T. Rozgonyi, P. Marquetand, and T. Weinacht, "Coherent control of internal conversion in strong-field molecular ionization," *Phys. Rev. Lett.* **125**, 053202 (2020).
31. I. J. Sola, E. Mével, L. Elouga, E. Constant, V. Strelkov, L. Poletto, P. Villorosi, E. Benedetti, J.-P. Caumes, S. Stagira, C. Vozzi, G. Sansone, and M. Nisoli, "Controlling attosecond electron dynamics by phase-stabilized polarization gating," *Nat. Phys.* **2**, 319-322 (2006).
32. M. Li, J.-W. Geng, H. Liu, Y. Deng, C. Wu, L.-Y. Peng, Q. Gong, and Y. Liu, "Classical-quantum correspondence for above-threshold ionization," *Phys. Rev. Lett.* **112**, 113002 (2014).
33. X. Song, C. Lin, Z. Sheng, P. Liu, Z. Chen, W. Yang, S. Hu, C. D. Lin, and J. Chen, "Unraveling nonadiabatic ionization and Coulomb potential effect in strong-field photoelectron holography" *Sci. Rep.* **6**, 28392 (2016).
34. D. G. Arbó, K. L. Ishikawa, K. Schiessl, E. Persson, and J. Burgdörfer, "Intracycle and intercycle interferences in above-threshold ionization: The time grating," *Phys. Rev. A* **81**, 021403 (2010).
35. F. Lindner, M. G. Schätzel, H. Walther, A. Baltuška, E. Goulielmakis, F. Krausz, D. B. Milošević, D. Bauer, W. Becker, and G. G. Paulus, "Attosecond Double-Slit Experiment," *Phys. Rev. Lett.* **95**, 040401 (2005).
36. W.-C. Jiang and X.-Q. Tian, "Efficient split-lanczos propagator for strong-field ionization of atoms," *Opt. Express* **25**, 26832-26843 (2017).
37. M. Liu, X.-Q. Wang, L. Jia, P.-G. Yan, and W.-C. Jiang, "Signatures beyond the rotating-wave approximation in retrieving the photoionization time delay from an ω - 2ω interferometric method," *Phys. Rev. A* **108**, 013102 (2023).
38. K. Amini, J. Biegert, F. Calegari, A. Chacón, M. F. Ciappina, A. Dauphin, D. K. Efimov, C. F. de Morisson Faria, K. Giergiel, P. Gniewek, A. S. Landsman, M. Lesiuk, M. Mandrysz, A. S. Maxwell, R. Moszyński, L. Ortmann, J. A. Pérez-Hernández, A. Picón, E. Pisanty, J. Prauzner-Bechcicki, K. Sacha, N. Suárez, A. Zair, J. Zakrzewski, and M. Lewenstein, "Symphony on strong field approximation," *Rep. Pro. Phys.* **82**, 116001 (2019).
39. L. Bai, J. Zhang, Z. Xu, and D.-S. Guo, "Photoelectron angular distributions from above threshold ionization of hydrogen atoms in strong laser fields," *Phys. Rev. Lett.* **97**, 193002 (2006).
40. Y. Huismans, A. Rouzée, A. Gijsbertsen, P. S. W. M. Logman, F. Lépine, C. Cauchy, S. Zamith, A. S. Stodolna, J. H. Jungmann, J. M. Bakker, G. Berden, B. Redlich, A. F. G. van der Meer, K. J. Schafer, and M. J. J. Vrakking, "Photoelectron angular distributions from the ionization of xenon rydberg states by midinfrared radiation," *Phys. Rev. A* **87**, 033413 (2013).